ELSEVIER

Chemical Engineering Journal 140 (2008) 22–31

Chemical Engineering Journal

www.elsevier.com/locate/cej

Prediction of the spray scrubbers' performance in the gaseous and particulate scrubbing processes

P. Keshavarz, Y. Bozorgi, J. Fathikalajahi *, M. Taheri

Chemical and Petroleum Engineering Department, College of Engineering, Shiraz University, Shiraz, Iran

Received 26 October 2005; received in revised form 22 August 2007; accepted 28 August 2007

Abstract

In this study, the spray scrubber's performance in its two classical applications, i.e. gaseous pollutants scrubbing and aerosol removing processes has been simulated by developing two proper mathematical models. The droplets dynamic behavior has been modeled in the Lagrangian framework in which the PSI-Cell model has been applied to obtain the droplets concentration in each tower increment. In order to apply the Lagrangian approach, a mathematical model has been presented for the classical pressure nozzles. One of the unique advantages of the models is their capability to predict the liquid film formation. Moreover, the droplet size distribution and especially the nozzles' real locations have been incorporated into the models and their probable effects have been investigated. The effects of liquid film formation on both the gaseous and particulate scrubbing efficiency have been probed as well. After validation of the model by some experimental data from the literature, the effect of different parameters such as nozzle locations, nozzle jet velocity and other parameters have been explained.

Keywords: Spray scrubber; Gaseous scrubbing; Particulate scrubbing

1. Introduction

Spray scrubbers are one of the most commonly used types of equipment for a wide variety of applications in industry. This is probably because of their simple design and low pressure drop (operating cost), while the main drawback of using this equipment is sludge disposal.

There are three simultaneous conditioning effects for this equipment: gas cooling and humidification, gaseous scrubbing and particle removal which correspond to the rain air-conditioning effects. As a brief literature survey for the two earlier applications, Hixon and Scott [1] examined the capability of the spray scrubbers in the absorption of various gases. There had been no previous attention paid to liquid film formation, droplet behavior and many other parameters in this equipment. Pigford and Pyle [2] performed the first elaborate experimental study on the spray types of towers in the gaseous scrubbing process. Many parameters such as liquid film formation, size distribution of the droplets discharged from the solid and hollow cone nozzles, and some other parameters were also measured. Sharma and Mehta [3] investigated the mass transfer operation in this equipment. Although the liquid film formation was ignored, they underlined that this parameter most probably does have a substantial effect on the scrubber performance. Michalski [4] presented a dynamic model for the droplets motion in the spray systems; but droplet motion is regarded to be one-dimensional, so it is unable to predict liquid film formation. Brogen and Karlsson [5] studied SO_2 absorption with liquid lime using the penetration theory. In addition to the assumption of the average diameter for the droplets, liquid film has been overlooked. Makkinejad [6] presented the various parameters effects on both closed and open loop pilot plant spray scrubber temperature profiles. Rahimi et al. [7] developed momentum, mass and especially energy balance to obtain the temperature profile in the hot gas spray scrubbers in two cement plants. But like Makkinejad, the droplets dynamic behavior and the spray system performance were not considered.

A few notable studies exist for the particle removing process in this equipment [8]. In other words, this application of spray scrubbers is not well known and has not been focused. This is perhaps because of the problem of sludge. Both a typical cyclone and a spray scrubber have pressure drops of the same order of magnitude [9,10]. Both can efficiently handle coarse particles, more or less, but the cyclone does not have the sludge problems

* Corresponding author. Tel.: +98 711 2303071; fax: +98 711 6287294.
E-mail address: zeglda@shirazu.ac.ir (J. Fathikalajahi).

1385-8947/$ – see front matter © 2007 Elsevier B.V. All rights reserved.
doi:10.1016/j.cej.2007.08.034

Nomenclature

C_D	drag coefficient
$C_P(D_p, z)$	concentration of particle size D_p in the zth increment of the tower (kg/m^3)
D	droplet diameter (m)
D_p	particle diameter (m)
D_t	tower diameter (m)
f	correction factor for the pressure nozzle jet flow uniformity
frac	fraction of the droplets changed into liquid film at any moment
$F_d(\theta_i, D_j)$	flow rate of the droplets corresponding to the droplets size D_j discharged from the ith angular increment of the cone or nozzle (kg/s)
$F_{dL}(\theta_i, D_j)$	flow rate of droplets converting into liquid film corresponding to the droplets size D_j discharged from ith angular increment from the cone or nozzle (kg/m^2 s)
F_g	gas flow rate (kg/s)
F_L	liquid flow rate (kg/s)
g	gravity acceleration (m/s^2)
k	constant
K_{gd}	overall mass transfer coefficient between the droplets and the gas (kg/m^2 s)
K_{gL}	overall mass transfer coefficient between the liquid film and the gas (kg/m^2 s)
Num (j, z)	number of droplets size j at zth increment
ΔP	pressure drop (Pa)
Q_g	gas flow rate (m^3/s)
Q_t	total liquid volume flow rate (m^3/s)
r	radial direction
R	tower radius
Re	Reynolds number
Sc	Schmitt number
Sh	Sherwood number
v_e	equivalent velocity (m/s)
v_g	gas velocity (m/s)
v_r	r-direction velocity (m/s)
v_z	z-direction velocity (m/s)
x_j	number fraction of the jth droplet size
X_d	pollutant concentration in the droplets (kg/m^3)
X_L	pollutant concentration in the liquid film (kg/m^3)
Y_g	gas phase concentration (kg/m^3)
Y_g^*	concentration of the gaseous pollutant (ammonia) in equilibrium with the water phase.
z_{max}	the last increment of the tower height

Greek letters

η	target efficiency
ρ_g	gas density (kg/m^3)
ρ_L	liquid density (kg/m^3)

Subscripts

d	droplet
i	angle index
in	inlet
j	droplet index
out	outlet
P	particle

(disposal, treating, recovery, etc.). So, from this consequential viewpoint, cyclones are superior to spray scrubbers.

Nevertheless, particle removal is one of the consequent and inherent prospects of any scrubbing system, as, in some circumstances, this equipment is used for particle removing processes. For example, it is used as a conditioner of the ammonium nitrate laden air in the Shiraz Petrochemical Complex, ammonium nitrate second unit [11]. It is necessary to indicate that this equipment is efficient in treating particles larger than 2 μm [9].

The objective of this research is to provide a parallel survey and assessment of the performance of spray scrubbers in both gaseous and particulate scrubbing processes. The models are validated by the data of Pigford and Pyle [2] and Pilat et al. [8], respectively. Not only are the models capable of predicting liquid film formation, but the nozzles real locations and the droplet size distribution have also been incorporated into them and their probable effects have been probed (it is also necessary to indicate that the presented method for the prediction of the liquid film formation, by taking the nozzles' real locations into account, can also be used to predict the liquid film formation at any kind of scrubber with any nozzle arrangement). Likewise, the effects of liquid film formation on the efficiency of both processes have been elucidated. In order to adopt the Lagrangian framework for the droplets, a conductive mathematical model has been presented for the classical pressure nozzles which can be used for any spray system.

2. Mathematical modeling

In this study, for both gaseous and particulate scrubbing, the Lagrangian method, which is based on tracking each individual discontinuous phase element (droplets), has been applied to estimate the droplets velocity profile in r and z directions. Subsequently, droplet trajectories are specified. In parallel, the PSI-Cell model, which is based on the simple system of counting, is used to calculate/count the droplets concentration/number, total specific area and total projected surface area (for the gaseous and particulate scrubbing, respectively) in each increment of the tower. However, the equations of mass transfer for gaseous scrubbing are quite different from the corresponding equations for particulate matters. This is due to the different nature of their transfer mechanisms.

In this work, like the previous ones, a plug flow has been assumed for the carrier gas (air), and no relative velocity has been assumed between the pollutant matter and the carrier gas—the gaseous pollutant dissolves in the carrier gas. Also, for a typical

particle size of 5 μm subjected to a typical velocity of 1 m/s, the drag force is much greater than the particle gravity force. In other words, and as a whole, no significant relative velocity exists between the carrier gas and the two types of pollutants.

Moreover, it is assumed that no liquid film re-entrainment occurs, as this is a customary phenomenon in high-energy scrubbers [12]. This assumption has been made due to the low velocity of the gas in the various spray types of scrubbers.

One of the main issues in the modeling of high-energy scrubbers (high pressure drop or velocity), like any type of orifice scrubber, is the turbulancy of the gas. Mohebbi et al. [13,14], in the modeling of an orifice scrubber, incorporated the turbulancy effects (eddies) into the particles governing equations because the particles were very small (about 0.5 μm) and also the gas velocity was more than 60 m/s. But the effect of eddies on the droplets was ignored because the inertia of the droplets was more than 300 times higher than that of the particles [13,14]. But in this study, like the previous studies, the effects of probable eddy for both particles and droplets were ignored. This approach is justified because the particles treated in a spray scrubber are normally much larger than those of orifice types (that is why the amount of pressure drop needed in the spray scrubbers is much lower than that of orifice types). Also the gas velocity in the spray types is much lower than that of the orifice types. In addition, the droplet size distribution in the spray types is much larger than those of the orifice because the droplets in the spray types are generated by the nozzles, while in the orifice types, the droplets are generated (atomized) by a gas with a very high speed (one can compare the droplet size distribution published by Pigford and Pyle [2] for the spray scrubbers with what is given by Alenso et al. for venturi scrubbers [15]). So as a whole, it is a reliable assumption to ignore the eddy effects on the droplets and particles in the spray scrubbers. In the following sections, the two models for gaseous and particulate scrubbing are presented, respectively.

2.1. Gaseous scrubbing

By applying the mass balance on a cylindrical control volume for the carrier gas and the droplets, and also on a shell-shaped control volume for the liquid film, the solute (gaseous pollutant) concentration profile in the three mentioned mediums will be obtained according to the following sections.

2.1.1. Mass transfer for the carrier gas phase

The gas phase flow rate depends on the mass transfer operation with the droplet and liquid film phases. Therefore

$$\frac{\mathrm{d}(F_\mathrm{g})}{\mathrm{d}z} = \sum_0^i \sum_1^j \frac{6}{D_j} \frac{F_\mathrm{d}(\theta_i, D_j)}{\rho_\mathrm{L} v_z(\theta_i, D_j)} K_\mathrm{gd}(Y_\mathrm{g} - Y_\mathrm{g}^*) + K_\mathrm{gL}(Y_\mathrm{g} - Y_\mathrm{g}^*)\pi D_\mathrm{t} \quad (1)$$

$$\frac{\mathrm{d}(Y_\mathrm{g} F_\mathrm{g})}{\mathrm{d}z} = \sum_0^i \sum_1^j \frac{6}{D_j} \frac{F_\mathrm{d}(\theta_i, D_j)}{\rho_\mathrm{L} v_z(\theta_i, D_j)} K_\mathrm{gd}(Y_\mathrm{g} - Y_\mathrm{g}^*) + K_\mathrm{gL}(Y_\mathrm{g} - Y_\mathrm{g}^*)\pi D_\mathrm{t} \quad (2)$$

Y_g^* stands for the concentration of the gaseous pollutant (ammonia) in the air in equilibrium with the corresponding concentration in the water phase.

2.1.2. Mass transfer for the droplet phase

The droplets flow rate, at any section of the tower, is dependent on the amount of liquid film formation and the amount of pollutant transferred to the droplet phase. So

$$\frac{\mathrm{d}F_\mathrm{d}(\theta_i, D_j)}{\mathrm{d}z} = \sum_0^i \sum_1^j \frac{6}{D_j} \frac{F_\mathrm{d}(\theta_i, D_j)}{\rho_\mathrm{l} v_z(\theta_i, D_j)} K_\mathrm{gd}(Y_\mathrm{g}(\theta_i, D_j) - Y_\mathrm{g}^*) - F_\mathrm{dL}(\theta_i, D_j)\pi D_\mathrm{t} \quad (3)$$

$$\frac{\mathrm{d}(X_\mathrm{d}(\theta_i, D_j)F_\mathrm{d}(\theta_i, D_j))}{\mathrm{d}z} = \sum_0^i \sum_1^j \frac{6}{D_j} \frac{F_\mathrm{d}(\theta_i, D_j)}{\rho_\mathrm{l} v_z(\theta_i, D_j)} K_\mathrm{gd}(Y_\mathrm{g}(\theta_i, D_j) - Y_\mathrm{g}^*) - F_\mathrm{dL}(\theta_i, D_j)X_\mathrm{d}\pi D_\mathrm{t} \quad (4)$$

2.1.3. Mass transfer for the liquid film phase

The liquid film flow rate is dependent on the amount of droplets which change into liquid film and also the amount of pollutant transferred to it. Therefore

$$\frac{\mathrm{d}F_\mathrm{L}}{\mathrm{d}z} = \sum_0^i \sum_1^j \pi D_\mathrm{t} F_\mathrm{dL}(\theta_i, D_j) + K_\mathrm{gL}\pi D_\mathrm{t}(Y_\mathrm{g} - Y_\mathrm{g}^*) \quad (5)$$

$$\frac{\mathrm{d}(X_\mathrm{L}F_\mathrm{L})}{\mathrm{d}z} = \sum_0^i \sum_1^j X_\mathrm{d}(\theta_i, D_j)\pi D_\mathrm{t} F_\mathrm{dL}(\theta_i, D_j) + K_\mathrm{gL}\pi D_\mathrm{t}(Y_\mathrm{g} - Y_\mathrm{g}^*) \quad (6)$$

It should be noted that in the previous studies, the nozzles' real locations were disregarded. In other words, the nozzles were assumed to be located at the center of the cross-section of the tower. Also, no angular (θ) direction was made for the droplets at any increment of the tower. But, by incorporation of the nozzles' real location, a profile in the θ direction is formed for any droplet size flow rate ($F_\mathrm{d}(\theta_i, D_j)$ or $F_\mathrm{dL}(\theta_i, D_j)$ in Eqs. (1)–(6) at any increment of the tower.

In order to solve Eqs. (1)–(6), the expressions of different types of mass transfer coefficient (K_gf and K_gL), the droplets velocity profile, and the droplets concentration (number) profile are needed, and so have been explained as follows.

2.1.4. Mass transfer coefficients

According to the results of Pigford and Pyle, the mass transfer resistance is embedded in the gas phase. One of the most popular equations for the gas-droplet mass transfer coefficient is the equation proposed by Frossling [16] to obtain the gas-droplet mass transfer coefficient (or gas phase mass transfer coefficient) as follows

$$Sh = 2 + 0.552 Re^{0.5} Sc^{0.33} \quad (7)$$

Also, the equation proposed by Treybal [17] has been used to calculate the gas–liquid film mass transfer coefficient as follows

$$Sh = 3.41. \tag{8}$$

2.1.5. Droplets velocity profile

By implementation of Newton's second law on the droplets and doing some arithmetic rearrangement, Eqs. (9) and (10) are obtained for the droplets velocity equations:

$$\frac{dv_z}{dz} = \frac{g(\rho_l - \rho_g)}{\rho_l |v_z|} - \frac{3C_D \rho_g |v_e|(|v_g| + |v_z|)}{4D|v_z|\rho_L} \tag{9}$$

$$\frac{dv_r}{dz} = -\frac{3C_D \rho_g |v_e||v_r|}{4D|v_z|\rho_L} \tag{10}$$

The drag coefficient is obtained by Calvert's equation [18]:

$$C_D = \frac{55}{Re_j} \tag{11}$$

It is necessary to indicate that square root normal distribution has been used to represent the droplet size distribution. This function has been recommended by Masters [19] for the distribution of the droplets size.

2.1.6. Droplets concentration profile

The particle source in cell (PSI-Cell) model, which is based on a simple system of counting, has been used to calculate the droplets number concentration in each segment of the tower. If the number flow rate of droplets at the starting location 0 is Num(0), the number flow rate of droplets size j is obtained by

$$\mathrm{Num}(j, 0) = x_j \mathrm{Num}(0) \tag{12}$$

Also, the number of droplets size j at zth increment is given as

$$\mathrm{Num}(j, z) = \frac{F_d(j, z)}{\rho_L \left(\pi D_j^3/6\right)} \tag{13}$$

The details of the PSI-Cell model are given elsewhere [20].

2.2. Particulate scrubbing

The mechanism of the particle removing process is quite different from that of the gaseous scrubbing one. While the specific area and the equilibrium concentration of the interested solute play key factors in the mass transfer operation in the gaseous scrubbing, the total projected surface area of the droplets and particles–droplets relative velocity are the main factors in the overall collection efficiency in the particle removing process. As a consequence, unlike the gaseous scrubbing process, the liquid film has no role in the particulate scrubbing because of having no significant projected area [21].

Like gaseous scrubbing, the differential mass balance on three engaged phases, i.e. gas, droplets and the liquid film are applied to obtain the pollutant (particles) concentration profiles in the corresponding phases.

2.2.1. Mass equations for the carrier gas phase

$$\frac{d(Q_g)}{dz} = \sum_{1}^{j}\sum_{0}^{i}\sum_{D_{p\min}}^{D_{p\max}} \eta(\theta_i, D_p, D_j)\frac{3}{2D_j} \times \frac{F_d(\theta_i, D_j)}{\rho_L |v_z(\theta_i, D_j)|}(|v_g| + |v_z(\theta_i, D_j)|)C_P(D_p, z) \tag{14}$$

$$\frac{d(Q_g C_P)}{dz} = \sum_{1}^{j}\sum_{0}^{i}\sum_{D_{p\min}}^{D_{p\max}} \eta(\theta_i, D_p, D_j)\frac{3}{2D_j} \times \frac{F_d(\theta_i, D_j)}{\rho_L |v_z(\theta_i, D_j)|}(|v_g| + |v_z(\theta_i, D_j)|)C_P(D_p, z) \tag{15}$$

2.2.2. Mass equations for the droplet phase

$$\frac{dF_d(\theta_i, D_j)}{dz} = \sum_{1}^{j}\sum_{0}^{i}\sum_{D_{p\min}}^{D_{p\max}} \eta(\theta_i, D_p, D_j)\frac{3}{2D_j} \times \frac{F_d(\theta_i, D_j)}{\rho_L |v_z(\theta_i, D_j)|}(|v_g| + |v_z(\theta_i, D_j)|)C_P(D_p, z) \tag{16}$$

$$\frac{dX_d(\theta_i, D_j)F_d(\theta_i, D_j)}{dz} = \sum_{1}^{j}\sum_{0}^{i}\sum_{D_{p\min}}^{D_{p\max}} \eta(\theta_i, D_p, D_j)\frac{3}{2D_j} \times \frac{F_d(\theta_i, D_d)}{\rho_L |v_z(\theta_i, D_d)|}(|v_g| + |v_z(\theta_i, D_j)|)C_P(D_p, z) \tag{17}$$

2.2.3. Mass equations for the liquid film phase

$$\frac{dF_L}{dz} = \sum_{1}^{j}\sum_{0}^{i}\sum_{D_{p\min}}^{D_{p\max}} F_{dL}(\theta_i, D_j)\pi D_t \tag{18}$$

$$\frac{d(X_L F_L)}{dz} = \sum_{1}^{j}\sum_{0}^{i}\sum_{D_{p\min}}^{D_{p\max}} X_d(\theta_i, D_j)F_{dL}(\theta_i, D_j)\pi D_t \tag{19}$$

In order to solve Eqs. (14)–(19), expressions of droplets velocity and concentration profiles, the target efficiency and overall collection efficiency are needed. The expressions for the droplets velocity and concentration are the same as those given previously for the gaseous scrubbing process and are not repeated here.

2.2.4. Target efficiency (η) and overall collection efficiency

The particle removing mechanism includes three coordinates: inertial impaction, interception and diffusion. Their corresponding equations are long so that one can find them elsewhere in detail [22].

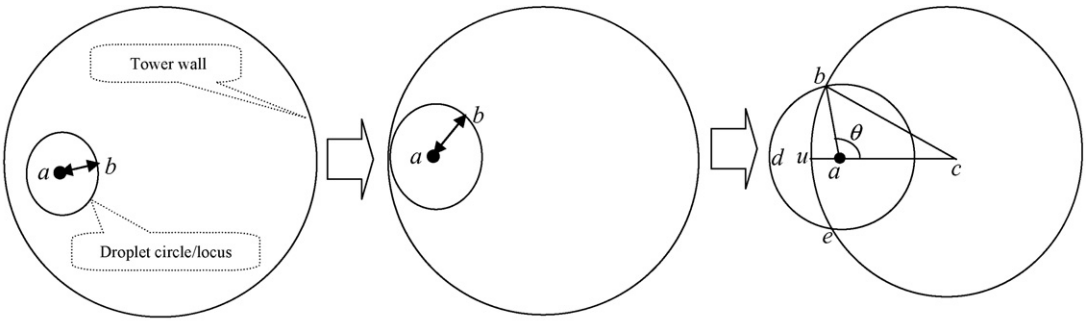

(a) The "droplets circle" is growing. Point "*a*" stands for the nozzle.

(b) The "droplets circle" has impacted the tower wall.

(c) *bde* arc is the fraction of the droplets which has been changed into the liquid film.

Fig. 1. Configuration of nozzle and droplet circle in a typical spray scrubber. (a) The "droplets circle" is growing. Point "*a*" stands for the nozzle. (b) The "droplets circle" has impacted the tower wall. (c) *bde* arc is the fraction of the droplets which has been changed into the liquid film.

Also, the overall collection efficiency is defined as the ration of the removed particles to the total amount of input:

$$\eta_{\text{Overall}} = 1 - \frac{\sum_{D_{\text{pmin}}}^{D_{\text{pmax}}} \int_0^R r v_{\text{g}} C_{\text{P}}(D_{\text{p}}, z_{\max})\,\text{d}r}{\sum_{D_{\text{pmin}}}^{D_{\text{pmax}}} \int_0^R r v_{\text{g}} C_{\text{P}}(D_{\text{p}}, 0)\,\text{d}r} \tag{20}$$

3. Evaluation of the liquid film formation

The droplets which have been discharged from a pressure nozzle move on a "growing circle" (from the top view) or inside a conical zone. This growing locus is small near the nozzle but gradually grows larger as the droplets fall down. Fig. 1a and b show this locus from the top view.

When this growing locus impacts the wall, the liquid film will be formed. For the liquid film formation calculation from the flow discharged from each nozzle at any section of the tower, the cosine rule has been used to obtain the droplets fraction which has been changed into the liquid film as follows (Fig. 1c)

$$(bc)^2 = (bc - ua)^2 + (ab)^2 - 2(bc - ua)(ab)\cos(\theta) \tag{21}$$

Note that the (*ab*) or the "droplets circle" radius is obtained by the droplets dynamic equations (Eqs. (9)–(11)). So the fraction of droplets which have been changed into the liquid film ($b\widehat{de}$) can be calculated as (Fig. 1c):

$$\text{frac} = \frac{2\pi - 2\theta}{2\pi} = \frac{b\widehat{de}}{2\pi} \tag{22}$$

Also, it is evident that:

$$\text{The flow rate of droplets size } D_{\text{j}} \text{ which have been converted into liquid film (kg/s)} = F_{\text{d}}(D_j) \times \text{frac} \tag{23}$$

So it is readily possible to obtain the amount of liquid film formation and also the total flow rate of liquid film at any section of the tower.

4. Mathematical modeling for the pressure nozzles

The flow from a classical type of a pressure nozzle is a cone shaped form [19]. Initially, we assume that the droplets are uniformly impacted on an imaginary surface below the nozzle point. So the droplet flow rate, at any height below the nozzle, can be obtained as

$$F_{\text{d}}(\theta_i) = kA(\theta_i), \quad 0 \le \theta_i \le \theta_{\max} \tag{24}$$

$A(\theta_i)$ is the total area blot out by the flow rate $F_{\text{d}}(\theta_i)$, and k is a constant which will be dropped from the equation later on. For total flow from the nozzle we have

$$F_{\text{dt}} = kA(\theta_{\max}) \tag{25}$$

For a cone type pressure nozzle, Eq. (24) can be rewritten as

$$F_{\text{d}}(\theta_i) = k\pi r^2(\theta_i) \tag{26}$$

Also according to Fig. 2, we have

$$\tan\left(\frac{\theta_i}{2}\right) = \frac{r}{h} \tag{27}$$

Consequently, a combination of the above equations leads to

$$F_{\text{d}}(\theta_i) = \pi h^2 k \tan^2\left(\frac{\theta_i}{2}\right) \tag{28}$$

According to the definition of a derivative, the derivative of $F_{\text{d}}(\theta_i)$, with respect to θ and some calculations, one finally obtains

$$F_{\text{d}}(\Delta\theta_i) = F_{\text{dt}} \frac{(\tan^2(\theta_i + (\Delta\theta_i/2))/2) - (\tan^2(\theta_i - (\Delta\theta_i/2))/2)}{\tan^2(\theta_{\max}/2)} \tag{29}$$

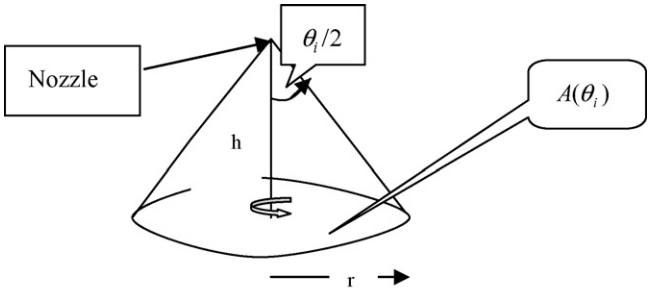

Fig. 2. A cone shaped jet flow.

where $F_d(\Delta\theta_i)$ is the flow rate of droplets between θ_i and $\theta_i + \Delta\theta_i$.

But in non-ideal cases, where droplet concentration is not uniform on the surface below the nozzle, a correction should be applied on Eq. (29). So an experimental parameter (f) should be applied for the calculation of the droplets flow rate at any angle. To evaluate this parameter, Pigford and Pyle [2] used some small cylindrical reservoirs 150 cm beneath the nozzles. According to them, if A is the cross-section area of one of these cylinders and θ is the angle from the cylinder center

$$F_d(\Delta\theta_i) = f(\theta_i) F_{dt} \Delta A(\theta_i) \frac{\cos^3(\theta_i/2)}{h^2} \tag{30}$$

Applying the same procedure used for the uniform case leads to the following equation:

$$F_d(\Delta\theta_i) = \pi F_{dt} f(\theta_i) \left[\tan^2\left(\frac{\theta_i + (\Delta\theta_i/2)}{2} \right) - \tan^2\left(\frac{\theta_i - (\Delta\theta_i/2)}{2} \right) \right] \cos^3\left(\frac{\theta_i}{2} \right) \tag{31}$$

By using Eq. (31), it is possible to calculate droplets which are injected in each angle accurately. $f(\theta_i)$ can be obtained from a simple experimental work such as Pigford and Pyle [2]. Eq. (31) can be used for any classical pressure nozzles to find the ejected droplets flow rates in each angle.

5. Numerical solution

In order to solve the suggested mass and momentum equations for both gaseous and particulate scrubbing, a cone element (because the droplets are discharged from the pressure nozzles in a cone shaped form) and also a droplet size are chosen. Then, the momentum equations are applied (Eqs. (9)–(11)) to obtain the elements/droplets different coordinates velocity, and subsequently, their corresponding trajectories. In parallel, Eqs. (21)–(23) assess if the droplet size in that specific element has impacted the wall or not. If impacted, it will be removed from the droplets flow and change into the liquid film. Otherwise, the PSI-Cell model (Eqs. (12) and (13)) calculates the droplets specific area and projected surface area (for gaseous and particulate scrubbing, respectively). This procedure will be applied to the other droplet sizes, cone, and tower height increments until all types of increments are covered. At the end, the droplets-specific and projected surface area and also velocity at any section of the tower are specified.

Subsequently, the droplets velocity and concentration matrices are inserted in the gas, droplets and liquid film mass equations to obtain the pollutants concentration profiles in all three phases for both gaseous (Eqs. (1)–(6)) and particulate (Eqs. (14)–(19)) scrubbing processes. The models solutions are performed with the Rung–Kutta 4th order method. A C++ code has been written to do the proposed sequences.

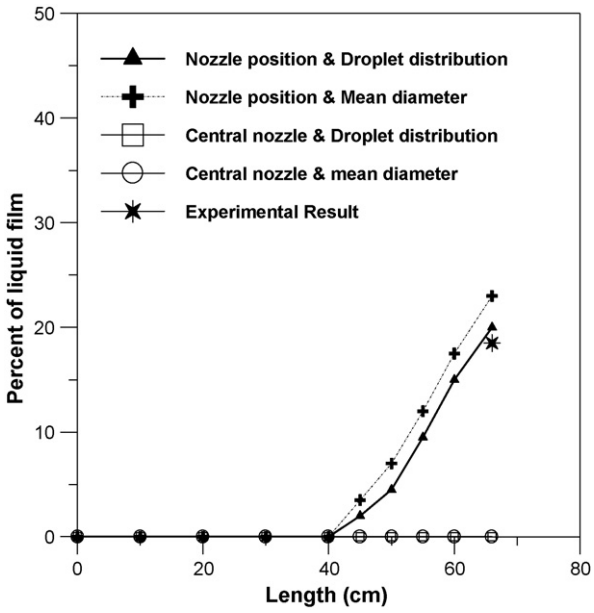

Fig. 3. Liquid film percentage vs. tower length in the 66 cm tower.

6. Results and discussion

In this section, the results for both gaseous and particulate scrubbing will be presented and discussed. The experimental data of Pigford and Pyle [2] and Pilat et al. [8] have been used to validate the models for the gaseous and particulate scrubbing processes, respectively.

6.1. Gaseous scrubbing

Fig. 3 presents the results of the current model (considering droplet size distribution and nozzles locations) and also three other different assumptions, implemented on the model for the prediction of the liquid film. The results obtained by these assumptions have been compared with the experimental data in a 66 cm tower. As is evident, in this spray scrubber, no liquid film has been predicted when it is assumed that all nozzles are located at the top center of the tower instead of their real position on a circular ring.

In "Nozzle position & Droplet distribution", both nozzles real locations and a droplet size distribution have been incorporated. In "Nozzle position & Mean diameter", the nozzles real locations have been considered, but a mean diameter has been used rather than a size distribution. In "Central nozzle & Droplet distribution" the nozzles are assumed to be located at the center of the cross-section of the tower, but a size distribution has been applied rather than a mean diameter. In the latest case, the nozzles real positions have been disregarded and also a mean diameter has been used rather than a droplet size distribution.

As expected, by considering nozzles position and droplet size distribution, better agreement has been acquired. Also as evident, the two latest cases (nozzles at center) predict no liquid film (their corresponding lines in Fig. 3 are tangent to the horizontal axis) which is evidently false according to the approximately 20% liquid film in the data. So in spray scrubbers modeling,

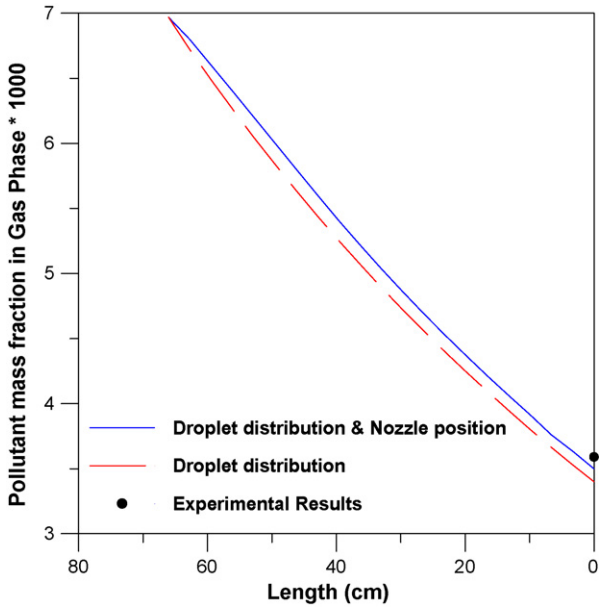

Fig. 4. Exit gas concentration of ammonia in the 66 cm tower.

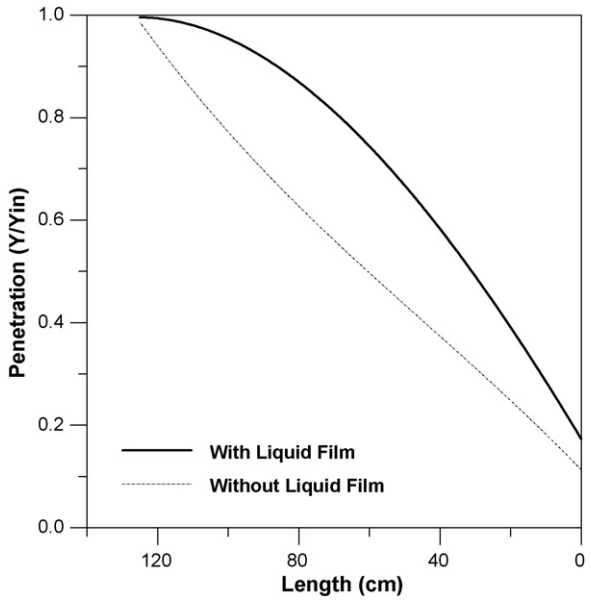

Fig. 6. Effect of liquid film disregarding in performance of gas spray scrubbers.

nozzle location can be very important and must be considered, especially for liquid film prediction.

Figs. 4 and 5 present the exit gas concentration by the indicated assumptions for two different scrubbers. It has been observed that the 'Droplet distribution & Nozzles position' exhibits the best agreement with the data, especially for the smaller tower.

As mentioned before, many investigators disregarded the liquid film formation in spray scrubbers. Fig. 6 shows that ignoring the liquid film formation in such an instrument can lead to a significant amount of error. According to this figure, the amount of error resulting from ignoring the liquid film formation will reduce when the height of the tower is increased. In the design of industrial spray towers, an effective liquid flow rate is normally considered to be one-fifth of the real flow rate [21]. Fig. 6 reveals that this fraction is not always true, especially when the tower is tall and the droplets have enough time to be saturated before contacting the tower wall.

Fig. 7 shows the simultaneous effects of gas relative solubility and liquid film formation on the absorption process in a 132 cm tower. The ammonia solubility in water is regarded as the basis gas. Y_{min} and Y_{out} stand for the pollutant exit concentration, while the liquid film formation has been ignored and considered, respectively. This figure shows that the assumption of no liquid

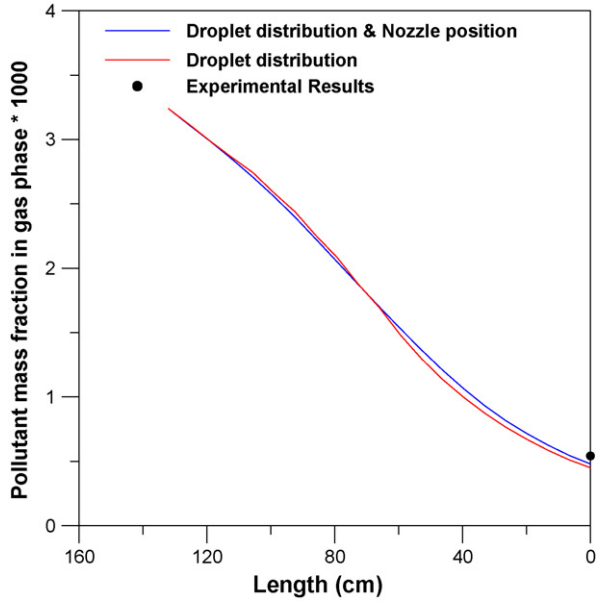

Fig. 5. Exit gas concentration of ammonia in the 132 cm tower.

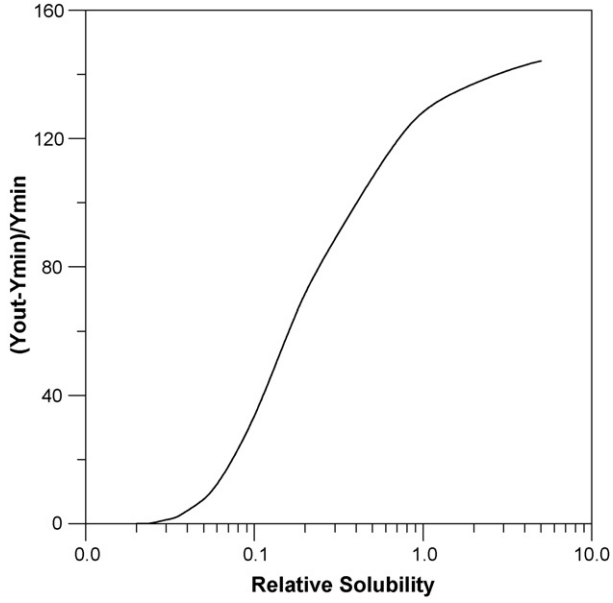

Fig. 7. Effect of the liquid film formation on the gaseous pollutant exit concentration vs. its relative solubility in the 132 cm tower.

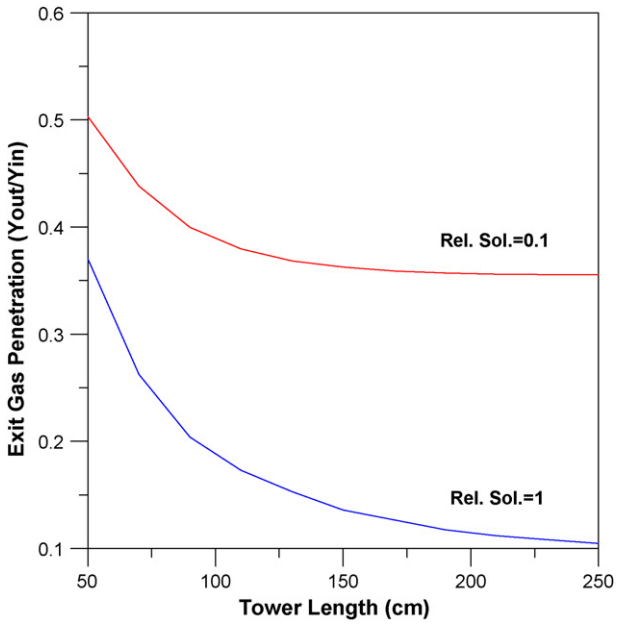

Fig. 8. Effect of the tower height on pollutants of different relative solubility exit concentration.

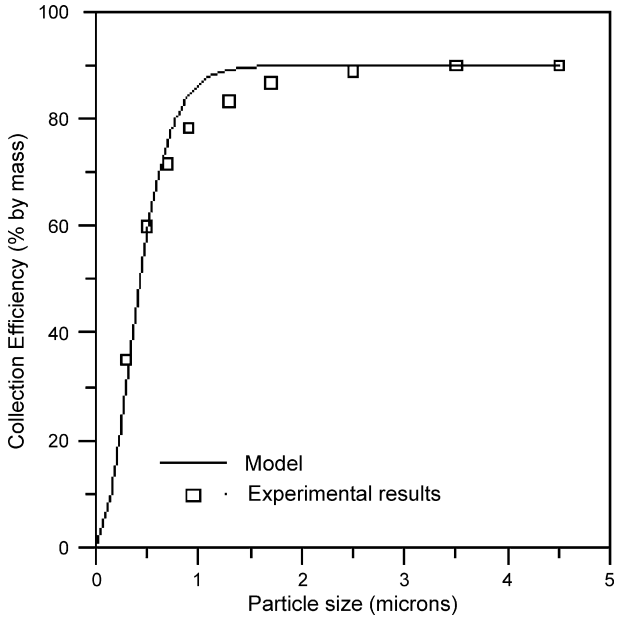

Fig. 10. The comparison between the model and experimental data (particulate scrubbing process).

film formation causes a smaller error for a pollutant with low solubility, because the droplets are nearly saturate before reaching the wall, and therefore, disregarding the liquid film formation does not affect the tower performance significantly.

Fig. 8 shows the effect of tower height on the absorption of two typical gaseous pollutants with different solubility in water. This figure also reveals that after a specific height, increasing the tower height has no influence on the absorption efficiency. Fig. 9 simultaneously demonstrates the effect of the tower diameter and height on the tower performance. It is evident that, as the tower diameter increases, the amount of liquid film formation decreases because the droplets have to move farther to impact the wall and convert into the liquid film.

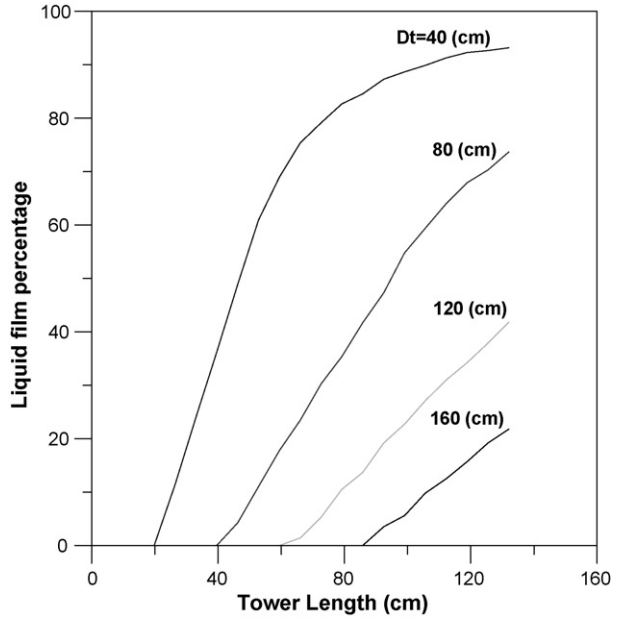

Fig. 9. Effect of the tower diameter and height on the formation of liquid film.

6.2. Particulate scrubbing

Fig. 10 compares the results obtained by the model for the collection efficiency of each particle cut size with data. As is obvious, a good agreement has been obtained.

Unfortunately, Pilat et al. did not report the nozzles real locations in their experimental studies. Nevertheless, we ourselves assumed three nozzles ways of arrangement in order to explore the effect of this parameter on the particulate collection efficiency (Fig. 11). In 'Without Nozzles Positions' nozzles are assumed to be located at the center of the tower. In 'With Nozzle Position (I)' the nozzles distance from the center of the tower is half of the distance from tower wall, but in 'With Nozzle Position (II)' this distance is two times more than the distance from the tower wall. As is evident from Fig. 11, the nozzles real location has no important effect on the prediction of the overall efficiency of the tower.

Fig. 12 demonstrates the effect of disregarding the liquid film formation on collection efficiency for each particle cut size. As is obvious, while the effect is relatively high for the tiny particles, no important effect emerges for large particles (E_2 and E_1 stand for the collection efficiency when liquid film formation has been ignored and incorporated, respectively). Nevertheless, as has been previously mentioned, the spray scrubber is used when the majority of particles are large; so that as whole, disregarding the liquid film formation does not significantly affect the particulate scrubbing performance.

Fig. 13 presents the effect of inlet nozzle velocity on collection efficiency. According to this figure, nozzle velocity has a very important effect in collection efficiency, especially for tiny particles with low efficiency. As indicated, increasing jet veloc-

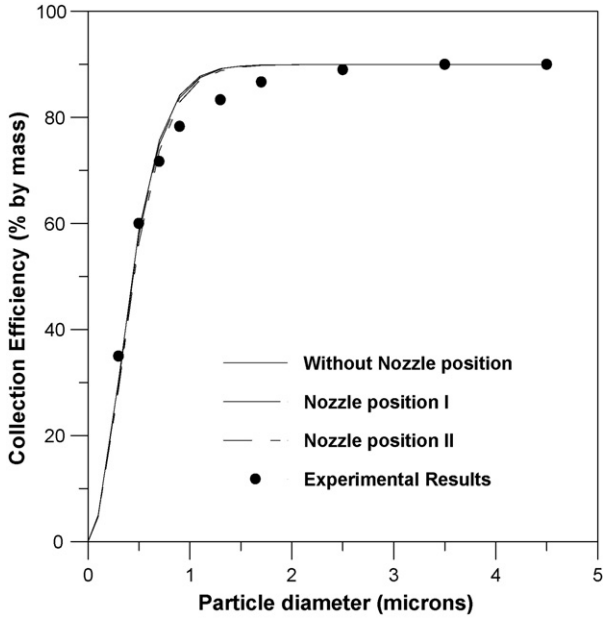

Fig. 11. Effect of nozzles' locations on each particle size collection efficiency.

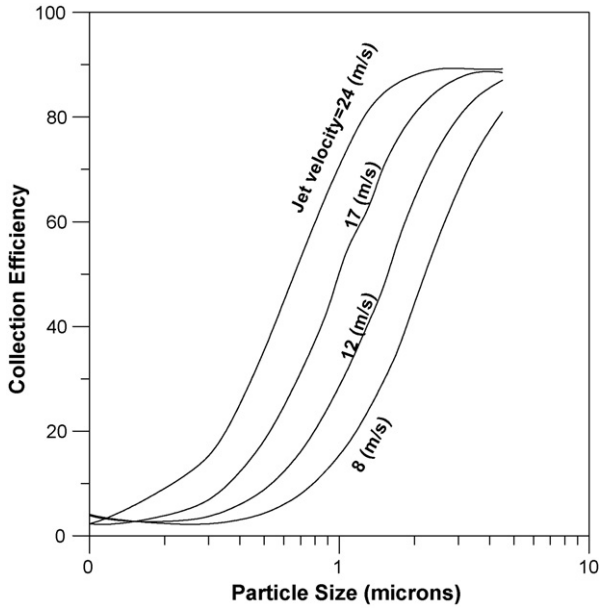

Fig. 13. Effect of jet velocity on collection efficiency.

ity from 8 to 24 m/s for 1 μm particles can raise efficiency from 15% to about 75%. This result can be important in the tower design.

Fig. 14 shows the effect of the tower diameter on the collection efficiency of each particle cut size. This figure reveals that increasing the tower diameter does not much influence the collection efficiency, and hence the overall collection efficiency. This is because most of the contributions of the particle removing phenomenon occur around the nozzles region where the relative velocity (particles and the droplets) is high. Consequently, farther distances contributions are small with respect to nozzles locations regions.

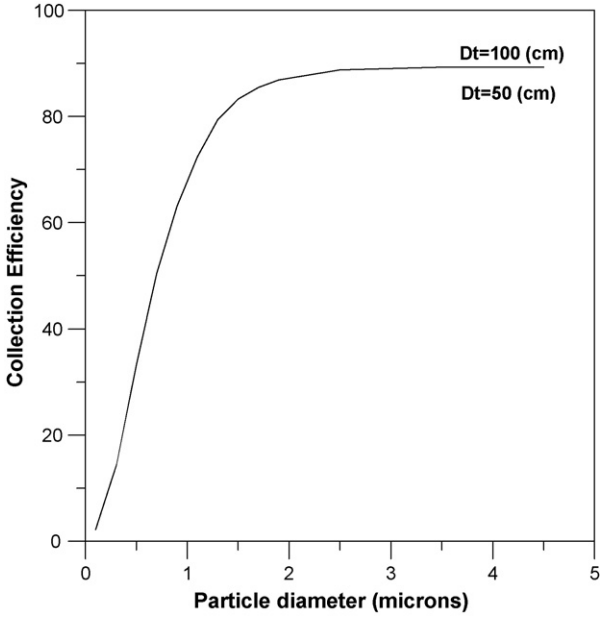

Fig. 14. Effect of the tower diameter on the collection efficiency of each particle cut size.

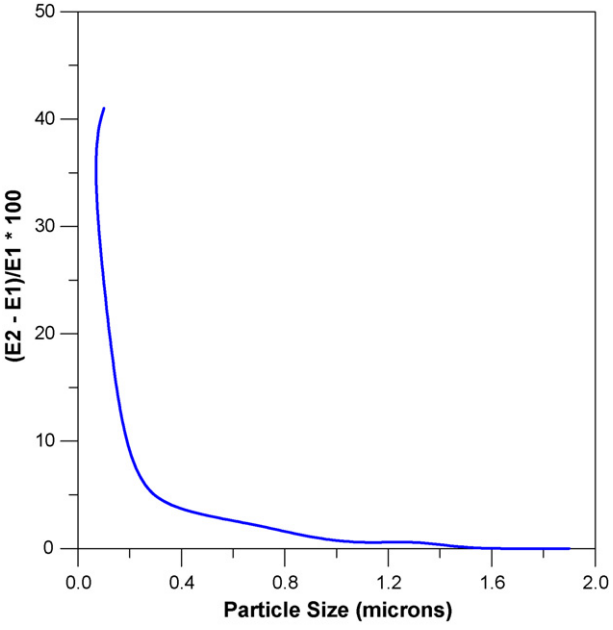

Fig. 12. Effect of ignoring the liquid film formation on the prediction of the collection efficiency.

7. Conclusion

The performance of the spray scrubber in both gaseous and particulate scrubbing processes has been simulated and the effects of several parameters have been studied. In particular, the liquid film formation and also the nozzles real locations have been investigated. It has been concluded that the nozzles real locations and liquid film formation can affect the spray scrubber performance significantly for gas scrubbing, while

the major factor influencing particle scrubbing is the inlet jet velocity.

References

[1] A.W. Hixon, C.E. Scott, Absorption of gases in spray towers, Ind. Eng. Chem. 27 (1935) 307.
[2] R. Pigford, C. Pyle, Performance characteristics of spray type absorption equipment, Ind. Eng. Chem. 43 (1951) 1649.
[3] M.P. Sharma, K. Mehta, Mass transfer in spray towers, Br. Chem. Eng. 15 (1970) 1440.
[4] J. Michalski, Aerodynamic characteristics of FGD spray towers, Chem. Eng. Technol. 20 (1997) 108.
[5] C. Brogen, H. Karlsson, Modeling the absorption of in a spray scrubber using the penetration theory, Chem. Eng. Sci. 52 (1997) 3085.
[6] N. Makkinejad, Temperature profile in countercurrent/cocurrent spray towers, Int. J. Heat Mass Transf. 44 (2000) 429.
[7] A. Rahimi, M. Taheri, J. Fathikaljahi, Mathematical modeling of heat and mass transfer in hot gas spray systems, Chem. Eng. Commun. 189 (2002) 959.
[8] M.J. Pilat, S.A. Jaasund, L.E. Sparks, Collection of aerosol particles by electrostatic droplet spray scrubbers, Environ. Sci. Technol. 8 (1974) 360.
[9] M.N. Rao, H.V.N. Rao, Air Pollution, 1st ed., McGraw-Hill Book Company, 2003.
[10] C.C. Lee, S.D. Lin, Handbook of Environmental Engineering Calculations, 1st ed., McGraw-Hill Book Company, 1999.
[11] Y. Bozorgi, Simulation of a Spray Scrubber in the Ammonium Nitrate Unit in Shiraz Petrochemical Complex, Thesis, Chemical and Petroleum Engineering Department, Shiraz University, April (2006).
[12] A. Rahimi, M. Taheri, J. Fathikaljahi, Mathematical modeling of non-isothermal venturi scrubbers, Can. J. Chem. Eng. 83 (2005) 1.
[13] M. Mohebbi, M. Taheri, J. Fathikaljahi, M.R. Talaie, Simulation of an orifice scrubber performance based on Eulerian/Lagrangian method, J. Hazard. Mater. A 100 (2003) 13.
[14] A. Mohebbi, M. Taheri, J. Fathikaljahi, M.R. Talaie, Prediction of pressure drop in an orifice based on Lagrangian approach, J. Air Waste Manage. Assoc. 52 (2002) 174.
[15] D.F. Alenso, J.A.S. Goncalves, B.J. Azzopardi, J.R. Coury, Drop size measurement in venturi scrubbers, Chem. Eng. Sci. 56 (2001) 4901.
[16] N. Frossling, Ueber die verdunstung fallender tropfen, Gerlands Batr. Geophys. 32 (1938) 170.
[17] R.E. Treybal, Mass Transfer Operation, 3rd ed., McGraw-Hill, 1980.
[18] S. Calvert, Venturi and other atomizing scrubbers efficiency and pressure drop, AIChE J. 16 (1970) 392.
[19] K. Masters, Spray Drying: An Introduction to Principles, Operational Particle and Applications, 2nd ed., John Wiley & Sons, New York, 1976.
[20] C.T. Crowe, M.P. Sharma, D.E. Stock, The particle source in cell (PSI-CELL) model for the gas-droplets flows, ASME, J. Fluids Eng. (1977) 325.
[21] C.D. Cooper, F.C. Alley, Air Pollution Control: A Design Approach, 2nd ed., Waveland Press, 1990.
[22] M. Crawford, Air Pollution Control Theory, 1st ed., McGraw-Hill Book Company, 1976.